Impact of electronic correlations on the equation of state and transport in ϵ-Fe

L. V. Pourovskii,[1,2] J. Mravlje,[3] M. Ferrero,[1] O. Parcollet,[4] and I. A. Abrikosov[2,5]

[1]*Centre de Physique Théorique, CNRS, École Polytechnique, 91128 Palaiseau, France*

[2]*Swedish e-science Research Centre (SeRC), Department of Physics, Chemistry and Biology (IFM), Linköping University, Linköping, Sweden*

[3]*Jozef Stefan Institute, SI-1000, Ljubljana, Slovenija*

[4]*Institut de Physique Théorique (IPhT), CEA, CNRS, URA 2306, F-91191 Gif-sur-Yvette, France*

[5]*Materials Modeling and Development Laboratory, National University of Science and Technology 'MISIS', 119049 Moscow, Russia*

(Received 12 December 2013; revised manuscript received 12 September 2014; published 16 October 2014)

We have obtained the equilibrium volumes, bulk moduli, and equations of state of the ferromagnetic cubic α and paramagnetic hexagonal ϵ phases of iron in close agreement with experiment using an *ab initio* dynamical mean-field-theory approach. The local dynamical correlations are shown to be crucial for a successful description of the ground-state properties of paramagnetic ϵ-Fe. Moreover, they enhance the effective mass of the quasiparticles and reduce their lifetimes across the $\alpha \rightarrow \epsilon$ transition, leading to a stepwise increase of the resistivity, as observed in experiment. The calculated magnitude of the jump is significantly underestimated, which points to nonlocal correlations. The implications of our results for the superconductivity and non-Fermi-liquid behavior of ϵ-Fe are discussed.

DOI: 10.1103/PhysRevB.90.155120 PACS number(s): 71.20.Be, 64.30.Ef, 71.27.+a, 72.15.Eb

I. INTRODUCTION

Understanding properly pressurized iron is important for the geophysics of Earth's inner core [1] as well as for technological applications of this metal. In the range of 12–16 GPa [2,3] a martensitic transition from the bcc ferromagnetic phase (α-Fe) to the hcp phase (ϵ-Fe) takes place. This ϵ-Fe phase, discovered in 1956 [4], exhibits surprising magnetic and electronic properties, including superconductivity in the range of pressures from 13 to 31 GPa with a maximum transition temperature of about 2 K[5] as well as a non-Fermi-liquid normal state observed in the same pressure range [6].

Perhaps the most puzzling aspect of ϵ-Fe is its magnetism, or, rather, the unexpected absence of it. Indeed, density-functional-theory (DFT) *ab initio* calculations within the generalized-gradient approximation (GGA) predict an antiferromagnetic ground state for the ϵ phase, with either collinear [7–9] or noncollinear [10] order, which has to date eluded experimental detection. While an anomalous Raman splitting observed in ϵ-Fe [11] has been related to a possible antiferromagnetic order [12], no magnetic splitting has been detected in this phase by Mössbauer spectroscopy down to temperatures of few Kelvin [13,14]. A collapse of the ordered magnetism across the α-ϵ transition has also been observed in the x-ray magnetic circular dichroism and in the x-ray absorption spectroscopy measurements [2]. A spin-fluctuation paring mechanism that has been proposed for the superconducting phase [15] also seems incompatible with the large-moment antiferromagnetism. If the nonmagnetic ground state is imposed, the DFT-GGA total energy calculations predict an equation of state that drastically disagrees with experiment. The bulk modulus is overestimated by more than 50%, and the equilibrium volume is underestimated by 10% compared to the experimental values [7]. Therefore, the ground-state properties of the observed nonmagnetic ϵ-Fe remain theoretically unexplained.

Another puzzling experimental observation is a large enhancement in the resistivity across the α-ϵ transition, with the room-temperature total resistivity of ϵ-Fe being twice as large as that of the α phase [16]. The electron-phonon-scattering contribution to resistivity calculated within GGA is in excellent agreement with the experimental total resistivity for the α phase [17]; however, these calculations predict virtually no change in the resistivity across the transition to antiferromagnetic hcp-Fe. The enhancement of resistivity in ϵ-Fe seems likely to be caused by the ferromagnetic spin fluctuations as the resistivity ρ follows $\rho \propto T^{5/3}$ [6,18]. This again is at odds with the antiferromagnetism suggested by the GGA calculations.

All of this points to the possible importance of the electronic correlations that are not correctly incorporated in the local or semilocal DFT. In this paper, we show that including local dynamical many-body effects significantly improves the description of iron. Within a local-density approximation plus dynamical mean-field theory (LDA+DMFT) framework we obtain the ground-state properties and the equation of states (EOS) of both ferromagnetic α and paramagnetic ϵ phases of iron as well as the α-ϵ transition pressure and volume change, in good agreement with experiment. The strength of the electronic correlations is significantly enhanced at the $\alpha \rightarrow \epsilon$ transition. This leads to a reduced binding, which explains the relatively low value of the measured bulk modulus in ϵ-Fe. The calculated resistivity has a jump at the transition, but the magnitude of the jump is severely underestimated compared with the experimental value, which points to additional scattering not present in our local approach.

Previously, the local correlations have been found to improve the description of the high-temperature paramagnetic α-Fe [19,20]. Moreover, the recently discovered electronic topological transition in ϵ-Fe has been successfully explained by LDA+DMFT but has not been captured within LDA and GGA [21]. However, no attempts to study ground-state and transport properties of ϵ-Fe within an LDA+DMFT approach have been reported to date.

II. METHOD

We have employed a fully self-consistent method [22,23] combining a full-potential band structure technique [24] and

LDA for the exchange/correlations with the DMFT [25] treatment of the on-site Coulomb repulsion between Fe 3*d* states. The Wannier orbitals representing Fe 3*d* states were constructed from the Kohn-Sham states within the energy range from −6.8 to 5.5 eV. The DMFT quantum impurity problem was solved with the numerically exact hybridization-expansion continuous-time quantum Monte Carlo (CT-QMC) method [26] using an implementation based on the TRIQS libraries [27] package. The local Coulomb interaction in the spherically symmetric form was parametrized by the Slater integral $F_0 = U = 4.3$ eV and Hund's rule coupling $J = 1.0$ eV chosen to reproduce a value of the ordered magnetic moment in α-Fe of $2.2\mu_B$ at its experimental volume. These values are somewhat larger than the values of $F_0 = U = 3.4$ eV and $J = 0.9$ eV obtained by the constrained-random-phase-approximation (cRPA) method in Ref. [28] for α-Fe. The 30% increase of U with respect to the static cRPA value accounts for the frequency dependence of the Coulomb vertex [29]. We used the around-mean-field form of the double-counting correction [30] in this work. We verified that the lowest-energy collinear antiferromagnetic order "AFM-II" [7] collapses at the largest experimental volume of ϵ-Fe in LDA+DMFT-CTQMC calculations with a rotationally invariant local Coulomb repulsion [31]. However, non-density-density terms in the Coulomb vertex dramatically increase the computational cost of CT-QMC and preclude reaching the high accuracy required to extract an equation of state. Hence, we adopted the paramagnetic phase for ϵ-Fe and employed the density-density approximation for the local Coulomb interaction throughout. This allowed us to use the fast "segment-picture" algorithm of the CT-QMC [26] and to reach an accuracy of about 0.5 meV/atom in the total energy computed in accordance with Ref. [23]. All our calculations were done for a relatively low temperature $T = 290$ K. Thus, the phonon and entropic contributions were neglected in the phase-stability calculations. The conductivity in DMFT is $\rho^{-1} = 2\pi e^2\hbar \int d\omega \sum_k -(\partial f/\partial\omega) v_k A_k(\omega) v_k A_k(\omega)$, with implicit summation over band indices [32]. We calculated the band velocities v_k using the WIEN2K optics package [24,33], and we constructed the spectral functions $A_k(\omega)$ from the highly precise DMFT self-energies (computed using 10^{11} CT-QMC moves), which we analytically continued to the real axis using Padé approximants.

III. EQUATION OF STATE AND ELECTRONIC CORRELATIONS

The obtained LDA+DMFT total energies vs volume in the α and ϵ phases are plotted in Fig 1(a). Our calculations predict the ferromagnetic bcc α phase to be the ground state. The transition to a paramagnetic ϵ-Fe [the common tangent shown in Fig 1(a)] is predicted to occur at a pressure P_c of 10 GPa. The paramagnetic α phase is about 10 mRy, or 1500 K higher in energy, in good correspondence to the Curie temperature of α-Fe. In Table I we list the resulting LDA+DMFT equilibrium atomic volumes and bulk moduli obtained by fitting calculated energy-volume data with the Birch-Murnaghan EOS [36]. Also shown are GGA lattice parameters and bulk moduli obtained by us and in previous works, as well as corresponding experimental values. The LDA+DMFT dramatically improves agreement with the experiment for paramagnetic ϵ-Fe for both the volume and bulk modulus, thus correcting the large overbinding error of GGA. The paramagnetic LDA+DMFT results are still closer to experimental values than the AFM GGA ones. Hence, even by adopting a magnetic state, which is not observed in experiment, one can only partially account for the influence of electronic correlations within the DFT-GGA framework. For α-Fe we obtain a relatively small correction to GGA, which already reproduces the experimental values quite well.

TABLE I. Equilibrium atomic volume V (a.u.^{3}/atom) and bulk modulus B (GPa) of bcc and hcp Fe computed by different *ab initio* approaches. The FM, PM, and NM subscripts indicate ferromagnetic, paramagnetic, and nonmagnetic states, respectively, and $AFM-II$ is the lowest-energy collinear magnetic structure of ϵ-Fe, in accordance with GGA calculations in Ref. [7]. LDA+DMFT values are from this work. GGA and experimental values are from (a) this work, (b) Ref. [34], (c) Ref. [9], (d) Ref. [7], and Ref. (e) [35].

bcc	LDA+DMFT$_{FM}$	GGA$_{FM}$	Expt.$_{FM}$
V	78.4	76.5,[a] 77.2,[b] 77.9[c]	78.9
B	168	187,[a] 174,[b] 186[c]	172

hcp	LDA+DMFT$_{PM}$	GGA$_{NM}$	GGA$_{AFM-II}$	Expt.
V	73.4	68.9,[a] 69[d]	71.2[d]	75.4[e]
B	191	288,[a] 292[d]	209[d]	165[e]

In Fig. 1(b) we compare the LDA+DMFT and GGA EOS with the one measured from Ref. [37]. Again, for both phases the LDA+DMFT approach successfully corrects the GGA overbinding error, which is relatively small in α-Fe and very significant in ϵ-Fe. Consequently, LDA+DMFT also reproduces correctly the volume change at the α-ϵ transition (about 5%), which is grossly overestimated in GGA. The c/a ratio in the hcp ϵ phase is also affected by the electronic correlations. As shown in Fig. 1(c), the GGA calculations predict a reduction of the c/a ratio with increasing volume, from 1.59 at $V = 58$ a.u.^{3}/atom to 1.58 at $V = 70$ a.u.^{3}/atom. Within LDA+DMFT the c/a ratio remains almost constant and is close to the value of 1.60, in good agreement with experimental measurements [38].

One may see that the ground-state properties (bulk modulus, equilibrium volume, etc.) of the ϵ phase are significantly modified within the LDA+DMFT approach compared to GGA. In contrast, for ferromagnetic α-Fe those modifications are much weaker. In order to understand the origin of this difference we have evaluated the strength of the correlation effects in both phases from the low-frequency behavior of the local DMFT self-energy $\Sigma(i\omega)$ on the Matsubara grid. Namely, we computed the average mass enhancement $\langle m^*\rangle/m_0$ as $\sum_s m_s^* N_s(E_F)/\sum_s N_s(E_F)$, where the s index designates combined spin and orbital quantum numbers $\{\sigma,m\}$, $\Sigma_s(i\omega)$ and $N_s(E_F)$ are the imaginary-frequency DMFT self-energy and partial density of states at the Fermi level for orbital s, respectively, and $m_s^* = 1 - [d\mathrm{Im}\Sigma_s(i\omega)/d\omega|_{\omega\to 0}]$ is the corresponding orbitally resolved mass enhancement. We have also evaluated the average inverse quasiparticle lifetime $\langle\Gamma\rangle = -\frac{m_0}{\langle m^*\rangle}\frac{\sum_s N_s(E_F)*\mathrm{Im}\Sigma_s(\omega=0)}{\sum_s N_s(E_F)}$. The resulting average mass enhancement and inverse quasiparticle lifetime are plotted in

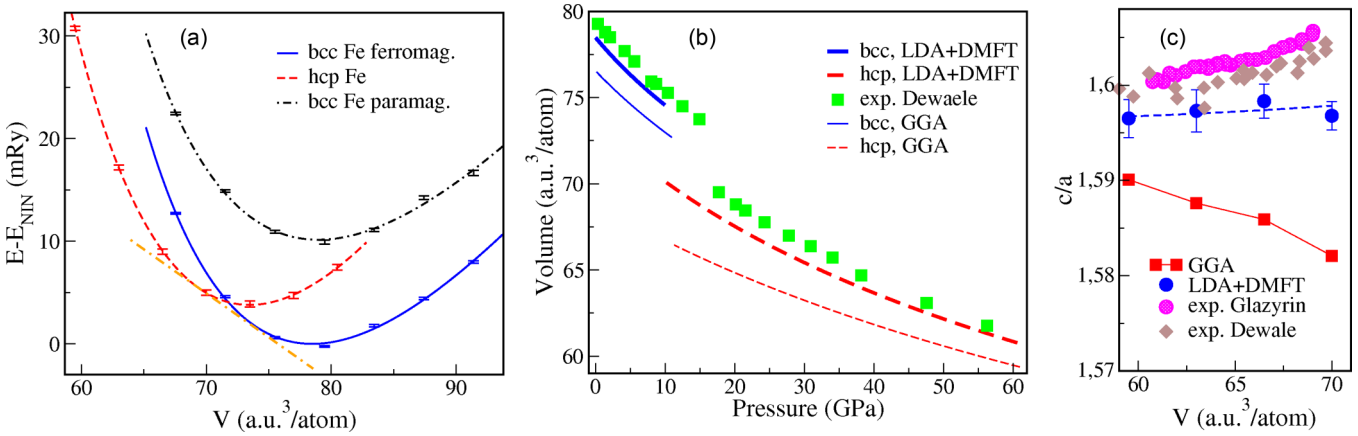

FIG. 1. (Color online) (a) LDA+DMFT total energy vs volume per atom for bcc (ferromagnetic, solid blue line, and paramagnetic, dot-dashed black line) and hcp (dashed red line) Fe. The error bars are the CT-QMC method stochastic error. The orange long-dash-dotted straight line indicates the common tangent construction for the α-ϵ transition. (b) EOS for ferromagnetic bcc (low pressure) and paramagnetic hcp (high pressure) Fe. Theoretical results are obtained by fitting the LDA+DMFT (thick line) and GGA (thin line) total energies using the Birch-Murnaghan EOS [36]. The experimental EOS of iron shown by green squares is from Dewaele *et al.* [37]. (c) The ratio of lattice parameters c/a of ϵ-Fe vs volume per atom obtained in LDA+DMFT (blue circles, dashed line) and GGA (red squares, solid line). The experimental data are from Dewaele *et al.* [37] (diamonds) and Glazyrin *et al.* [21] (pink circles).

Fig. 2. In ferromagnetic α-Fe both quantities slowly decay with decreasing volume, and then they exhibit a large enhancement across the α-ϵ transition, indicating a more correlated nature of ϵ-Fe. The latter is characterized by heavier quasiparticles, a larger electron-electron scattering, and a stronger volume dependence of the correlation strength compared to the bcc phase. This analysis clearly demonstrates that dynamical many-body effects are enhanced in the ϵ phase.

Why are the electronic correlations in ϵ-Fe stronger, and why does the DFT fail there? The crucial difference is the magnetism. In α-Fe, the physics is governed by the large static exchange splitting, which easily polarizes the paramagnetic state characterized by a peak in the density of states (DOS) close to the Fermi energy. Therefore, the spin-polarized DFT-GGA calculations, which are able to capture this static exchange splitting, reproduce the ground-state properties of ferromagnetic α-Fe rather well. Whereas in antiferromagnetic ϵ-Fe obtained within DFT-GGA the static exchange splitting also reduces the bonding and leads to an improved agreement with the experimental equation of state, the dynamical many-body effects must be included to describe the actual paramagnetic state of ϵ-Fe properly. In this respect we note that the many-body corrections to the total energy and spectral properties were shown to be important [20,39,40] for the high-temperature nonmagnetic state of α-Fe as well. If one suppresses magnetism, α-Fe is actually even more correlated than ϵ-Fe, which is a consequence of its large DOS close to the Fermi energy [41]. This larger DOS implies slower quasiparticles which are influenced by the interactions, especially the Hund's rule coupling [42].

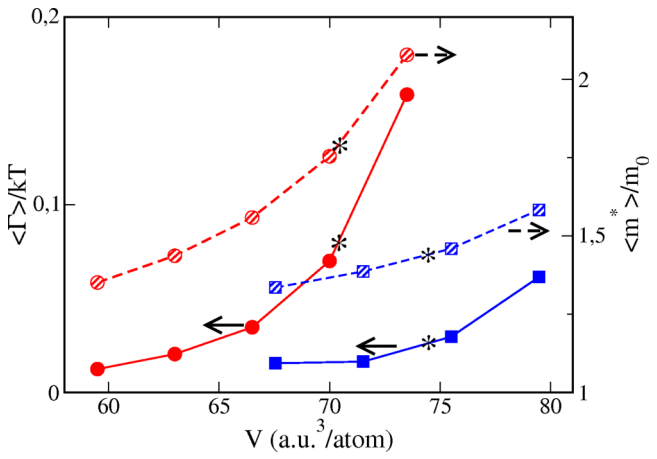

FIG. 2. (Color online) The ratio of the average inverse quasiparticle lifetime $\langle\Gamma\rangle$ to temperature (left axis) and the average mass enhancement $\langle m^*\rangle/m_0$ (right axis) vs volume per atom. The solid lines (solid symbols) and dashed lines (hatched symbols) are $\langle\Gamma\rangle/T$ and $\langle m^*\rangle/m_0$, respectively. The values for bcc and hcp phases are shown by blue squares and red circles, respectively. The black stars indicate the bcc and hcp atomic volumes at the transition point.

IV. TRANSPORT

We now turn to transport. The drop in the quasiparticle lifetime across the α-ϵ transition affects the electron-electron-scattering (EES) contribution to the resistivity $\rho_{\text{el.}-\text{el.}}$. We have calculated the evolution of the room-temperature $\rho_{\text{el.}-\text{el.}}$ versus pressure in both phases, as displayed in Fig. 3. One may see that the behavior of $\rho_{\text{el.}-\text{el.}}$ under pressure reflects that of the inverse quasiparticle lifetime Γ. The resistivity decays with pressure except at the transition point, where a stepwise increase is found. A rapid enhancement of $\rho_{\text{el.}-\text{el.}}$ in the ϵ phase at pressures below $P_c = 10$ GPa is in agreement with very recent measurements [43] in which a large hysteresis in the α-ϵ transition was obtained with the transition shifted to 7 GPa at the depressurization, and a very similar rapid increase in the total resistivity upon the decrease of pressure was observed in ϵ-Fe for pressures below the usual experimental P_c of 12–15 GPa.

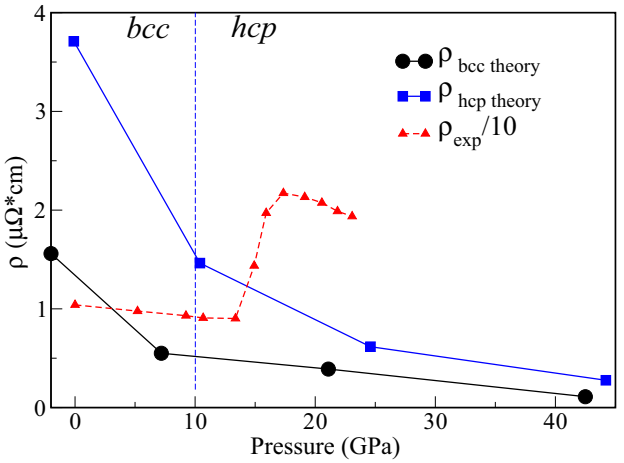

FIG. 3. (Color online) The electron-electron contribution to the resistivity in bcc α-Fe (black circles) and hcp ϵ-Fe (blue squares) computed within LDA+DMFT for $T = 294$ K. The experimental room-temperature resistivity divided by 10 [16] (red triangles, dashed line) is shown. The vertical dashed line indicates the theoretical transition pressure.

Now we discuss a very interesting point: despite the good qualitative agreement, the magnitude of the resistivity enhancement through the transition to ϵ-Fe in our calculations underestimates the values found in the experiment [16] by a factor of 10 (see Fig. 3 [44]). The calculations of the electron-phonon-scattering (EPS) contribution to resistivity in Ref. [17] reproduce the resistivity of the bcc-Fe well but exhibit almost no change across the transition. Therefore, the corresponding jump of the measured total resistivity has to be attributed to electron-electron scattering. If the experimental issues, such as sample thinning, can be excluded, then the missing scattering that we find in comparison with experiments has to be associated with the effects of nonlocal long-range correlations, which are not dealt with in our calculations. Interestingly, except for the magnitude, the pressure dependence of the resistivity is accounted well by our results. This might be understood by recognizing that the local correlations that suppress the coherence scale (the kinetic energy) also make the electronic degrees of freedom more prone to the effects of the coupling to the long-range spin fluctuations.

It is interesting to compare ϵ-Fe and Sr_2RuO_4, a widely investigated unconventional superconductor with a similar transition temperature [45], to make a further link with spin fluctuations. Both materials display low-temperature unconventional superconductivity [45], and several mechanisms have been discussed to be at its origin [46]. In Sr_2RuO_4 superconductivity emerges from a well-established Fermi liquid with $T_{FL} = 25$ K. Local approaches, like the one used in this work, yield much shorter lifetimes [47] and a resistivity which agrees with experiments at low temperatures within 30% [48]. The picture is different for ϵ-Fe, which displays a non-Fermi-liquid $T^{5/3}$ temperature dependence of its low-temperature resistivity [18], extending up to a temperature T^* which reaches the peak $T^*_{max} \approx 35$ K at a pressure where superconductivity reaches its maximum [43]. Spin fluctuations, which are believed to be responsible for this behavior [15], have, hence, a very strong effect on ϵ-Fe. Because their nonlocal nature cannot be captured within our framework, we believe that they are at the origin of the discrepancy between the experimental and our calculated resistivities.

V. SUMMARY

In summary, including local correlations crucially improves the theoretical picture of ϵ-Fe by correctly accounting for a set of experimental observations within the paramagnetic state. This solves the long-standing controversy between theory and experiment for this material. The successful description of ϵ-Fe within the paramagnetic state, together with an underestimation of the resistivity found in our local approach, hints at the importance of spin fluctuations, which supports scenarios relating the fluctuations to the origin of superconductivity.

ACKNOWLEDGMENTS

We are grateful to A. Georges and D. Jaccard for useful discussions. The input of X. Deng in the development of the transport code is gratefully acknowledged. A support provided by the Grant of Russian Federation Ministry for Science and Education (Grant No. 14.Y26.31.0005) and the Swedish Foundation for Strategic Research (SSF) program SRL Grant No. 10-0026 is gratefully acknowledged. L.P. acknowledges the travel support provided by PHD DALEN Project 26228RM. J.M. acknowledges the support of College de France, where a part of this work was done, and Slovenian Research Agency program P1-0044. O.P. acknowledges support from ERC under Grant No. 278472–MottMetals. The computations were performed on resources provided by the Swedish National Infrastructure for Computing (SNIC) at the National Supercomputer Centre (NSC) and PDC Center for High Performance Computing.

[1] S. Tateno, K. Hirose, Y. Ohishi, and Y. Tatsumi, Science **330**, 359 (2010).
[2] O. Mathon, F. Baudelet, J. P. Itié, A. Polian, M. d'Astuto, J. C. Chervin, and S. Pascarelli, Phys. Rev. Lett. **93**, 255503 (2004).
[3] A. Monza, A. Meffre, F. Baudelet, J.-P. Rueff, M. d'Astuto, P. Munsch, S. Huotari, S. Lachaize, B. Chaudret, and A. Shukla, Phys. Rev. Lett. **106**, 247201 (2011).
[4] D. Bancroft, E. L. Peterson, and S. Minshall, J. Appl. Phys. **27**, 291 (1956).
[5] K. Shimizu, T. Kimura, S. Furomoto, K. Takeda, K. Kontani, Y. Onuki, and K. Amaya, Nature (London) **412**, 316 (2000).
[6] P. Pedrazzini, D. Jaccard, G. Lapertot, J. Flouquet, Y. Inada, H. Kohara, and Y. Onuki, Phys. B (Amsterdam, Neth.) **378–380**, 165 (2006).

[7] G. Steinle-Neumann, L. Stixrude, and R. E. Cohen, Phys. Rev. B **60**, 791 (1999).

[8] G. Steinle-Neumann, R. E. Cohen, and L. Stixrude, J. Phys. Condens. Matter **16**, S1109 (2004).

[9] M. Friák and M. Šob, Phys. Rev. B **77**, 174117 (2008).

[10] R. Lizárraga, L. Nordström, O. Eriksson, and J. Wills, Phys. Rev. B **78**, 064410 (2008).

[11] S. Merkel, A. F. Goncharov, H.-K. Mao, P. Gillet, and R. J. Hemley, Science **288**, 1626 (2000).

[12] G. Steinle-Neumann, L. Stixrude, and R. E. Cohen, Proc. Natl. Acad. Sci. **101**, 33 (2004).

[13] G. Cort, R. D. Taylor, and J. O. Willis, J. Appl. Phys. **53**, 2064 (1982).

[14] A. B. Papandrew, M. S. Lucas, R. Stevens, I. Halevy, B. Fultz, M. Y. Hu, P. Chow, R. E. Cohen, and M. Somayazulu, Phys. Rev. Lett. **97**, 087202 (2006).

[15] I. I. Mazin, D. A. Papaconstantopoulos, and M. J. Mehl, Phys. Rev. B **65**, 100511 (2002).

[16] A. T. Holmes, D. Jaccard, G. Behr, Y. Inada, and Y. Onuki, J. Phys. Condens. Matter **16**, S1121 (2004).

[17] X. Sha and R. E. Cohen, J. Phys. Condens. Matter **23**, 075401 (2011).

[18] D. Jaccard and A. T. Holmes, Phys. B (Amsterdam, Neth.) **359–361**, 333 (2005).

[19] A. I. Lichtenstein, M. I. Katsnelson, and G. Kotliar, Phys. Rev. Lett. **87**, 067205 (2001).

[20] I. Leonov, A. I. Poteryaev, V. I. Anisimov, and D. Vollhardt, Phys. Rev. Lett. **106**, 106405 (2011).

[21] K. Glazyrin, L. V. Pourovskii, L. Dubrovinsky, O. Narygina, C. McCammon, B. Hewener, V. Schünemann, J. Wolny, K. Muffler, A. I. Chumakov *et al.*, Phys. Rev. Lett. **110**, 117206 (2013).

[22] M. Aichhorn, L. Pourovskii, V. Vildosola, M. Ferrero, O. Parcollet, T. Miyake, A. Georges, and S. Biermann, Phys. Rev. B **80**, 085101 (2009).

[23] M. Aichhorn, L. Pourovskii, and A. Georges, Phys. Rev. B **84**, 054529 (2011).

[24] P. Blaha, K. Schwarz, G. Madsen, D. Kvasnicka, and J. Luitz, *WIEN2k, An Augmented Plane Wave + Local Orbitals Program for Calculating Crystal Properties* (Technische Universitat Wien, Vienna, 2001).

[25] A. Georges, G. Kotliar, W. Krauth, and M. J. Rozenberg, Rev. Mod. Phys. **68**, 13 (1996).

[26] E. Gull, A. J. Millis, A. I. Lichtenstein, A. N. Rubtsov, M. Troyer, and P. Werner, Rev. Mod. Phys. **83**, 349 (2011).

[27] M. Ferrero and O. Parcollet, TRIQS, a toolbox for research on interacting quantum systems, http://ipht.cea.fr/triqs.

[28] T. Miyake, F. Aryasetiawan, and M. Imada, Phys. Rev. B **80**, 155134 (2009).

[29] M. Casula, P. Werner, L. Vaugier, F. Aryasetiawan, T. Miyake, A. J. Millis, and S. Biermann, Phys. Rev. Lett. **109**, 126408 (2012).

[30] M. T. Czyżyk and G. A. Sawatzky, Phys. Rev. B **49**, 14211 (1994).

[31] A. E. Antipov, I. S. Krivenko, V. I. Anisimov, A. I. Lichtenstein, and A. N. Rubtsov, Phys. Rev. B **86**, 155107 (2012).

[32] V. S. Oudovenko, G. Pálsson, K. Haule, G. Kotliar, and S. Y. Savrasov, Phys. Rev. B **73**, 035120 (2006).

[33] C. Ambrosch-Draxl and J. O. Sofo, Comput. Phys. Commun. **175**, 1 (2006).

[34] H. C. Herper, E. Hoffmann, and P. Entel, Phys. Rev. B **60**, 3839 (1999).

[35] H. K. Mao, Y. Wu, L. C. Chen, J. F. Shu, and A. P. Jephcoat, J. Geophys. Res. **95**, 21737 (1990).

[36] F. Birch, Phys. Rev. **71**, 809 (1947).

[37] A. Dewaele, P. Loubeyre, F. Occelli, M. Mezouar, P. I. Dorogokupets, and M. Torrent, Phys. Rev. Lett. **97**, 215504 (2006).

[38] The peculiarity in the c/a ratio in ϵ-Fe discussed in Ref. [21] cannot be resolved in our calculations. It is an order of magnitude smaller than the error bars due to CT-QMC stochastic error.

[39] A. A. Katanin, A. I. Poteryaev, A. V. Efremov, A. O. Shorikov, S. L. Skornyakov, M. A. Korotin, and V. I. Anisimov, Phys. Rev. B **81**, 045117 (2010).

[40] L. V. Pourovskii, T. Miyake, S. I. Simak, A. V. Ruban, L. Dubrovinsky, and I. A. Abrikosov, Phys. Rev. B **87**, 115130 (2013).

[41] R. Maglic, Phys. Rev. Lett. **31**, 546 (1973).

[42] A. Georges, L. de'Medici, and J. Mravlje, Annu. Rev. Condens. Matter Phys. **4**, 137 (2013).

[43] C. S. Yadav, G. Seyfarth, P. Pedrazzini, H. Wilhelm, R. Černý, and D. Jaccard, Phys. Rev. B **88**, 054110 (2013).

[44] Note that Fig. 2 suggests quite long scattering lifetimes. The transport scattering time τ_{tr} is an average of $-1/[2\mathrm{Im}\Sigma(\omega)]$ over the window opened by the Fermi function. For ϵ-Fe at $T =$ 295 K one obtains $\tau_{tr} \approx 80$ fs.

[45] A. P. Mackenzie and Y. Maeno, Rev. Mod. Phys. **75**, 657 (2003).

[46] Y. Maeno, S. Kittaka, T. Nomura, S. Yonezawa, and K. Ishida, J. Phys. Soc. Jpn. **81**, 011009 (2012).

[47] J. Mravlje, M. Aichhorn, T. Miyake, K. Haule, G. Kotliar, and A. Georges, Phys. Rev. Lett. **106**, 096401 (2011).

[48] J. Mravlje (unpublished).